2D protrusion but not motility predicts growth factor–induced cancer cell migration in 3D collagen

Aaron S. Meyer,[1,2] Shannon K. Hughes-Alford,[1,2] Jennifer E. Kay,[1,2] Amalchi Castillo,[1] Alan Wells,[3] Frank B. Gertler,[2] and Douglas A. Lauffenburger[1,2]

[1]Department of Biological Engineering and [2]Koch Institute for Integrative Cancer Research, Massachusetts Institute of Technology, Cambridge, MA 02139
[3]Department of Pathology University of Pittsburgh Medical Center, Pittsburgh, PA 15261

Growth factor–induced migration is a critical step in the dissemination and metastasis of solid tumors. Although differences in properties characterizing cell migration on two-dimensional (2D) substrata versus within three-dimensional (3D) matrices have been noted for particular growth factor stimuli, the 2D approach remains in more common use as an efficient surrogate, especially for high-throughput experiments. We therefore were motivated to investigate which migration properties measured in various 2D assays might be reflective of 3D migratory behavioral responses. We used human triple-negative breast cancer lines stimulated by a panel of receptor tyrosine kinase ligands relevant to mammary carcinoma progression. Whereas 2D migration properties did not correlate well with 3D behavior across multiple growth factors, we found that increased membrane protrusion elicited by growth factor stimulation did relate robustly to enhanced 3D migration properties of the MDA-MB-231 and MDA-MB-157 lines. Interestingly, we observed this to be a more reliable relationship than cognate receptor expression or activation levels across these and two additional mammary tumor lines.

Introduction

In most all solid cancers, dissemination of cells and establishment of distant metastases is an essential step in disease mortality (Lazebnik, 2010). Dissemination of carcinomas occurs by invasion across a basement membrane layer and migration through interstitial matrix to blood or lymph vessels. Efficient migration in this context requires coordinate regulation of cytoskeletal protrusion, adhesion, proteolysis, and contraction (Lauffenburger and Horwitz, 1996; Friedl and Wolf, 2009), each of which is modulated by paracrine and autocrine growth factor cues.

Cell migration has principally been studied as translocation across rigid 2D substrata. Despite the relevance of migration within ECM to tumor progression (Wolf et al., 2009) and known qualitative and quantitative differences in cell movement between 2D and 3D environments (Zaman et al., 2006; Doyle et al., 2009; Fraley et al., 2010), analysis of cells embedded within the ECM remains relatively uncommon because of technical difficulty and incompatibility with most biochemical analyses. Functional genomic screening techniques have been used to identify regulators of cell migration in planar contexts (Simpson et al., 2008; Lara et al., 2011), and analogous efforts were used to identify small molecule drug targets (Yarrow et al., 2005) or ascertain dependence on key signaling pathways (Wolf-Yadlin et al., 2006). The physiological relevance of results obtained from such high-throughput efforts is related directly to the degree that cellular responses measured in 2D systems correlate to those within ECM environments. Determining whether in fact any metrics easily obtained from 2D assays correlate robustly with 3D migration behavior across a broad range of treatment conditions is therefore critical.

We herein address this challenge for the important case of breast carcinoma cell migration. Through quantitative analysis of motility across multiple triple-negative (estrogen receptor [ER]−/progesterone receptor [PR]−/HER2 normal) breast carcinoma cell lines moving in 3D within collagen I matrix, we evaluate the predictive value of measurements, such as receptor expression, and motility surrogates, such as cell translocation in 2D. We fail to observe correlation between growth factor–induced motility responses on either stiff or compliant ECM in a 2D context and those within 3D ECM.

Correspondence to Douglas A. Lauffenburger: lauffen@mit.edu

Abbreviations used in this paper: DIC, differential interference contrast; EGFR, EGF receptor; ER, estrogen receptor; GAPDH, glyceraldehyde 3-phosphate dehydrogenase; PR, progesterone receptor; RMS, root mean squared.

The Rockefeller University Press $30.00
J. Cell Biol. Vol. 197 No. 6 721–729
www.jcb.org/cgi/doi/10.1083/jcb.201201003

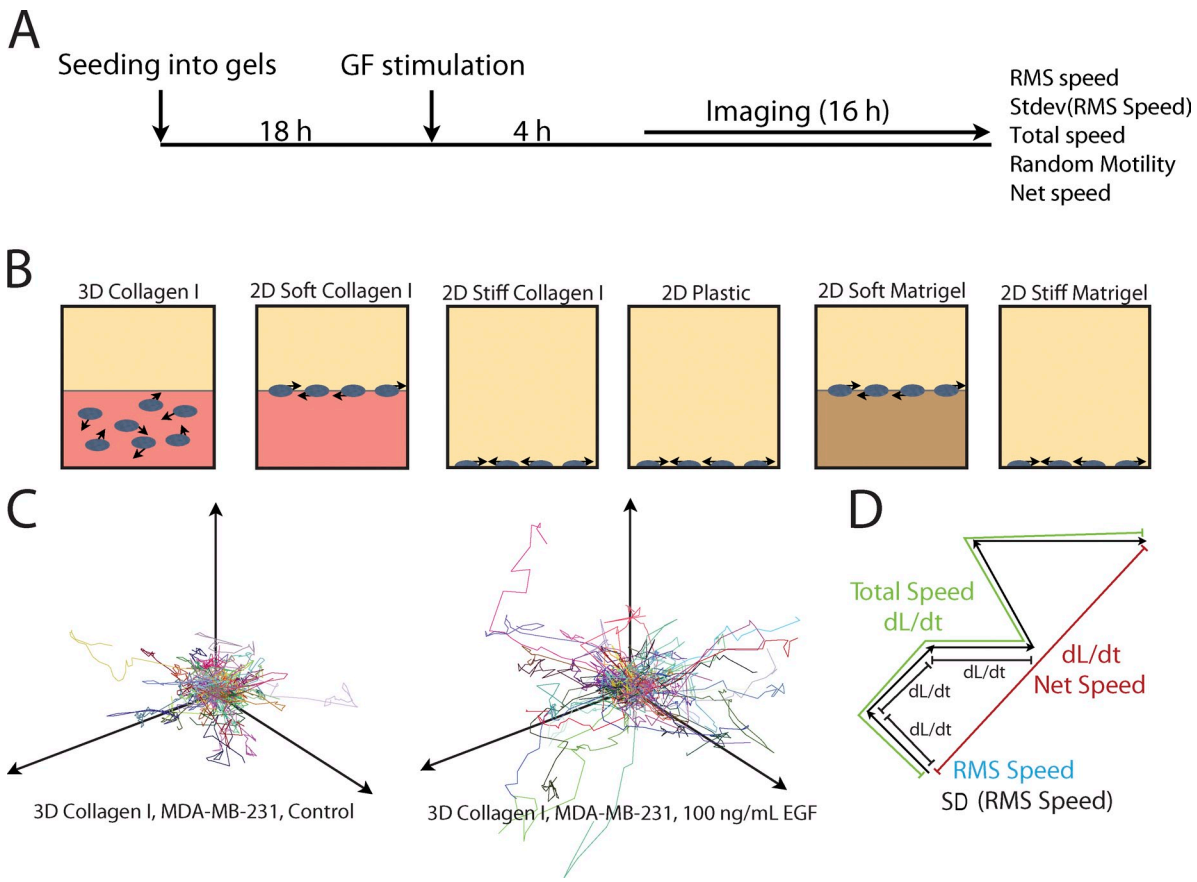

Figure 1. **Schematic of the migration assays.** (A) Schematic of the migration assay protocol. (B) Cells were seeded on or in matrix or on plastic for 18 h before growth factor stimulation. 4 h after growth factor stimulation, cells were imaged for 16 h. Arrows show cell movement. (C and D) Tracks of each cell were produced (C) and used to calculate five parameters summarizing the migration phenotype of each cell (D). dL/dt, change in length over time.

Although cognate receptor expression can weakly predict the relative motility responses across cell lines, it fails to quantitatively predict motility enhancement caused by growth factor stimulation. By examination of individual migration-related biophysical processes, we identify that acute lamellipodial protrusion dynamics of cells in response to growth factor cues can predict motility within 3D ECM. These findings have broad consequence in the assessment of motility responses in vitro, both for high-throughput experiments and for deeper investigation of how growth factor–elicited signaling network activities govern migration behavior.

Results and discussion

Systematic quantification of migration

To address multicomponent responses to growth factor stimulation, we performed a battery of quantitative single-cell migration assays using multiple human breast tumor cell lines and assay geometries (see Materials and methods; Fig. 1, A and B). Cells were fluorescently labeled to facilitate image analysis, and their displacement was tracked via live-cell microscopy over the course of 16 h in the presence or absence of seven growth factor cues relevant to the tumor microenvironment (Fig. 1 C and Fig. S1, A and B; Mograbi et al., 1997; Hankinson et al., 1998; Dunn et al., 2004; Cheng et al., 2005, 2008; Goswami et al., 2005; Hutcheson et al., 2007; Pasanisi et al., 2008; McIntyre et al., 2010; Tyan et al., 2011; Wilson et al., 2011). Semiautomatic centroid tracking was used to extract multiple parameters that describe the migration phenotype of each cell. Each individual cell track provides five distinctly quantifiable properties (Fig. 1 D): (1) a root mean squared (RMS) speed of each time interval; (2) the variance of that speed; (3) a total speed calculated as the total path length normalized by the time of the experiment; (4) a net speed or the net displacement normalized by the duration of the experiment; and (5) a random motility coefficient calculated by fitting to a random walk model (Kipper et al., 2007). The migration parameters were independent of position within the gel, and cells were not biased in their direction of migration, indicating homogenous physical characteristics (Kim et al., 2008) and that the growth factors had distributed fairly uniformly throughout the gels before the observation period. Of 10 breast carcinoma cell lines investigated across clinical markers and subtypes, five were observed to migrate robustly (Table S1). Vimentin expression and subtype classification distinguished cells that did or did not migrate in 3D.

Initial analysis of the full dataset by multidimensional reduction techniques illustrated that speed (RMS speed and total speed) and persistence (net speed and random motility) broadly cluster into two groups (Fig. S1 C). This multidimensional

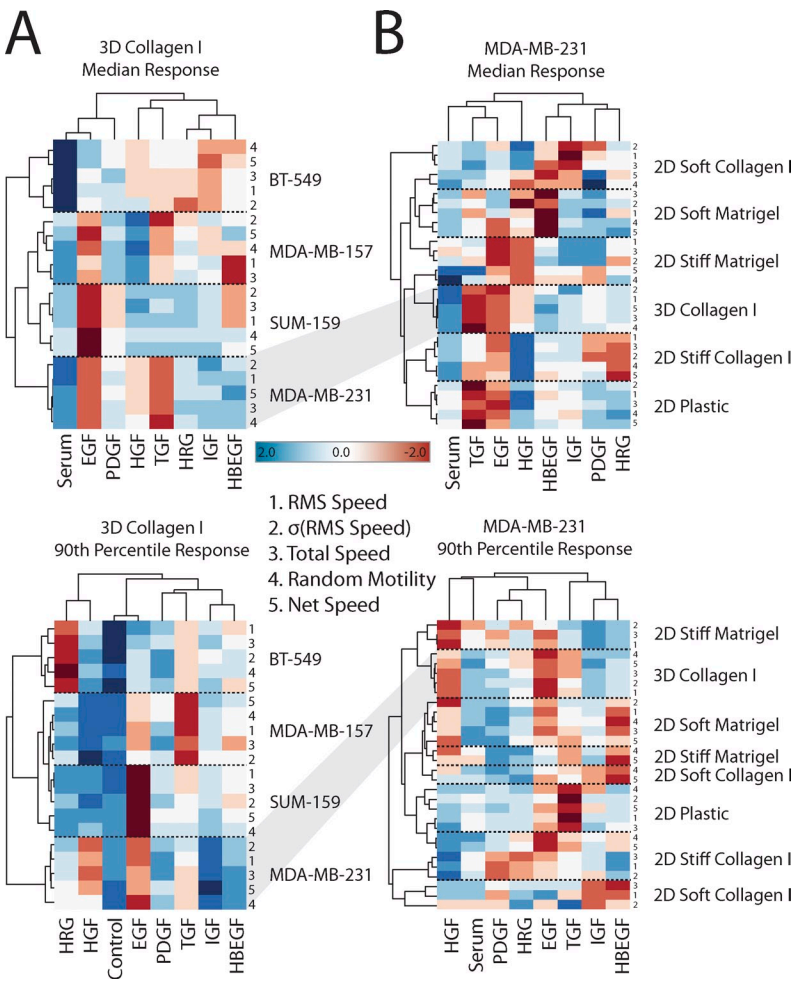

Figure 2. **Large-scale quantification of migration responses enables systems analysis of migration.** (A and B) Shown are mean-centered motility responses across eight growth factor conditions and four cell lines within collagen I gels (A) or MDA-MB-231 cells across different 2D and 3D motility assays (B; also see Fig. 1 B). Each profile and growth factor is clustered by rank correlation and mean linkage. Both the median (top) and 90th quantile (bottom) responses are shown as well as each migration metric (indicated by numbers). IGF, insulin-like growth factor 1; HRG, Heregulin β1; HBEGF, heparin-binding EGF-like growth factor; HGF, hepatocyte growth factor.

scaling seeks to preserve distance as a description of relative difference between each motility metric and indicates that cell speed and persistence are distinct parameters to describe migration captured by the assay. Using unsupervised clustering techniques, cell lines (Fig. 2 A) and dimensionalities or ECM in 2D (Fig. 2 B) were found to be separable. Weaker clustering among speed- or persistence-related motility metrics from identical cell lines or geometries was obtained, consistent with single cell–based clustering (Fig. S1 C). In some cases, distinguishable responses were observed when analyzing different quantiles of the single-cell migration metrics (Fig. S1 D), resulting in different response profiles (Fig. 2). Analysis of "outlier" cell populations is particularly important in invasive disease, as bulk population responses may not reflect disease etiology (Bernards and Weinberg, 2002; Al-Hajj et al., 2003; Cristofanilli et al., 2004; Weigelt et al., 2005). One important advantage of our large single-cell migration parameter dataset is the ability to quantify differences in responses within distinct cell subpopulations across assay conditions.

Prediction of motility enhancement by receptor expression

We tested the ability of growth factor receptor expression to predict differential motility response upon stimulation, as receptor expression is widely used to define clinical breast tumor subtype. Total protein expression was measured for three different growth factor receptors, which were implicated in breast cancer invasion and metastasis (Charafe-Jauffret et al., 2006; Jin and Esteva, 2008; Mader et al., 2011), in 2D for each cell line (Fig. 3 B), and every pairwise comparison of receptor expression and motility enhancement in 3D was performed (Fig. 3 A). With 24 comparisons (4× C(4,2)), ≥17 trials must correspond between receptor expression and motility for this relationship to be considered significantly predictive ($P < 0.05$). The analysis revealed a weak, but significant, association for three of four motility properties, with 15–18 correct associations (Fig. 3 C). Normalizing the measured properties for each cell line across the range of growth factor treatment conditions by variance, which may potentially account for differences among cell lines in their intrinsic motility capabilities, slightly improved the predictive capacity of receptor expression to 16–20 correct associations (Fig. 3 C). As receptor activation might have improved predictive capacity overexpression, we additionally tested the ability of EGF receptor (EGFR) pan-pY measurements to predict EGF and TGF-α motility enhancement (Fig. 3 E). Both stimulations may be directly compared in this case, resulting in 28 (C(8,2)) comparisons. Receptor activation, although distinct from expression, was not a better predictor of motility enhancement (Fig. 3 F).

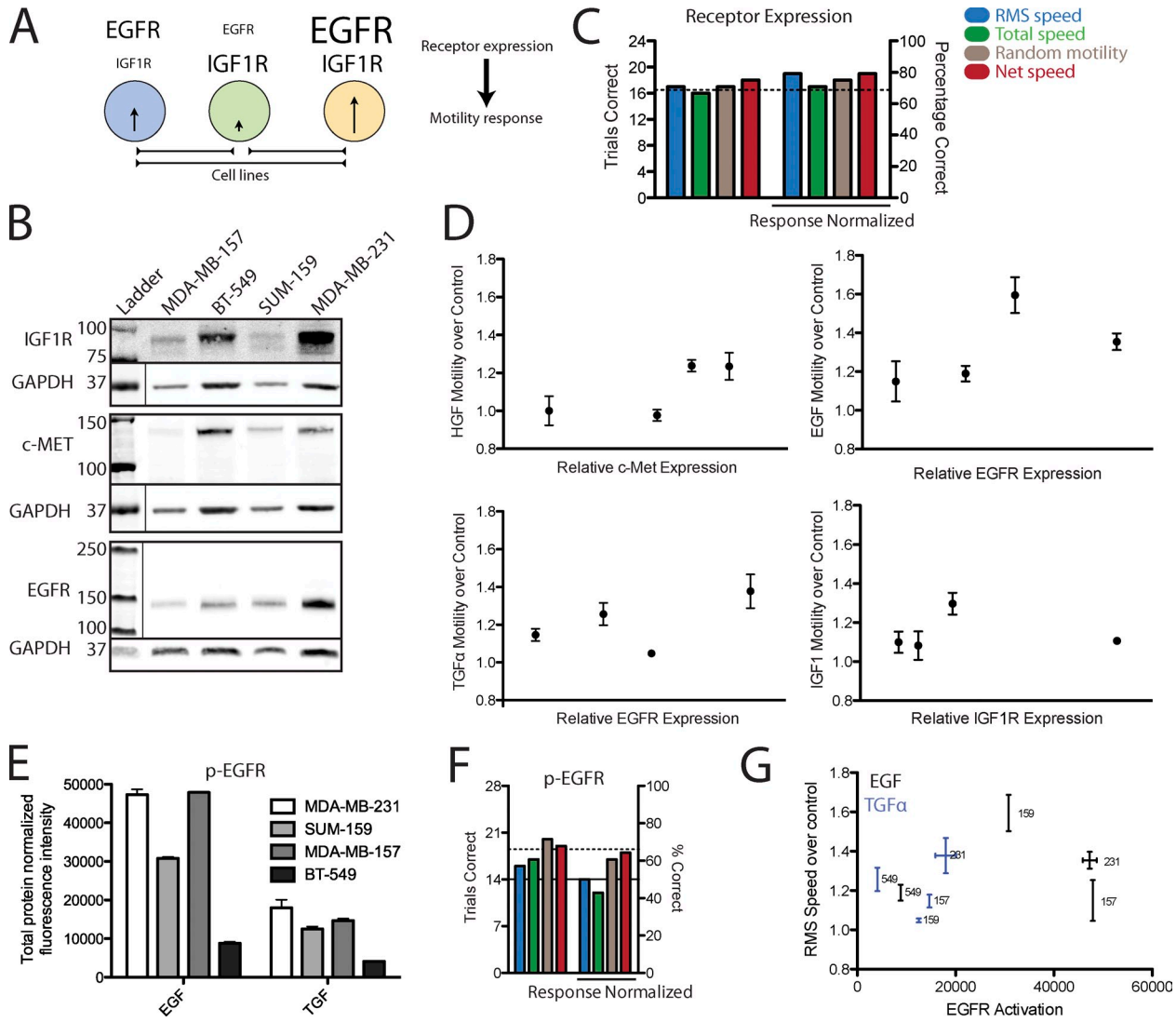

Figure 3. **Cognate receptor measurement is weakly informative of relative growth factor motility enhancement.** (A) Illustration of the pairwise comparison of receptor measurement and motility enhancement made between each cell line. (B) EGFR, IGF1R, and c-Met expression was measured across four cell lines. Lines separate loading controls from a different portion of the same membrane. Thin lines indicate portions of a membrane shown from a separate channel on the same membrane, position, and scan. (C) Every pairwise comparison of receptor expression and motility enhancement was made between cell lines for each metric of motility. Additionally, the motility enhancement for each cell line across all growth factor conditions was used to normalize for differences in the ability of each cell line to globally respond by migrating. The left and right y axes indicate the number and percentage of correct comparisons, respectively. Significance was tested by use of the binomial distribution (dotted line, $P < 0.05$). Migration measurements are the mean of at least three independent experiments. (D) Plots of RMS speed enhancement upon receptor stimulation versus relative receptor expression. Error bars indicate SEM from at least three independent experiments. (E) EGFR pan-pY measurement in cells stimulated with either EGF or TGF-α for 5 min. Error bars indicate the range of duplicate measurements. (F) Similar pairwise comparison analysis using measurement of p-EGFR to predict migration response. Migration measurements are the mean of at least three independent experiments. The continuous line indicates the maximum likelihood outcome of random chance. The dotted line indicates the $P < 0.05$ threshold. (G) Plot of RMS speed enhancement upon EGFR stimulation versus EGFR pan-pY measurement. Vertical error bars indicate SEM of at least three independent experiments; horizontal error bars indicate the range of duplicate measurements. Numbers refer to different cell lines.

Receptor expression levels thus predicted growth factor–elicited motility enhancement to a small degree that barely reached statistical significance. Although this provides support that receptor expression can account for some of the variation observed among cell lines and presumably among tumors, it is manifest that receptor expression or activation levels do not readily explain disparities in relative or absolute growth factor–enhanced migration responses (Fig. 3, D and G). Therefore, although expression measurements across many samples may indicate etiologically important changes, measurement of receptor expression alone within tumor cells will likely not be sufficient to identify the particular growth factor cues driving invasion and metastasis in the context of myriad heterogeneities among various samples.

Growth factor motility responses are distinct in 2D and 3D

Migration across a planar substratum has been the principal means for quantitative studies of responses to compound and genetic manipulations intended to inhibit metastasis (Simpson et al., 2008; Lara et al., 2011). Dissimilarities in unstimulated migration between 2D and 3D have been noted (Doyle et al.,

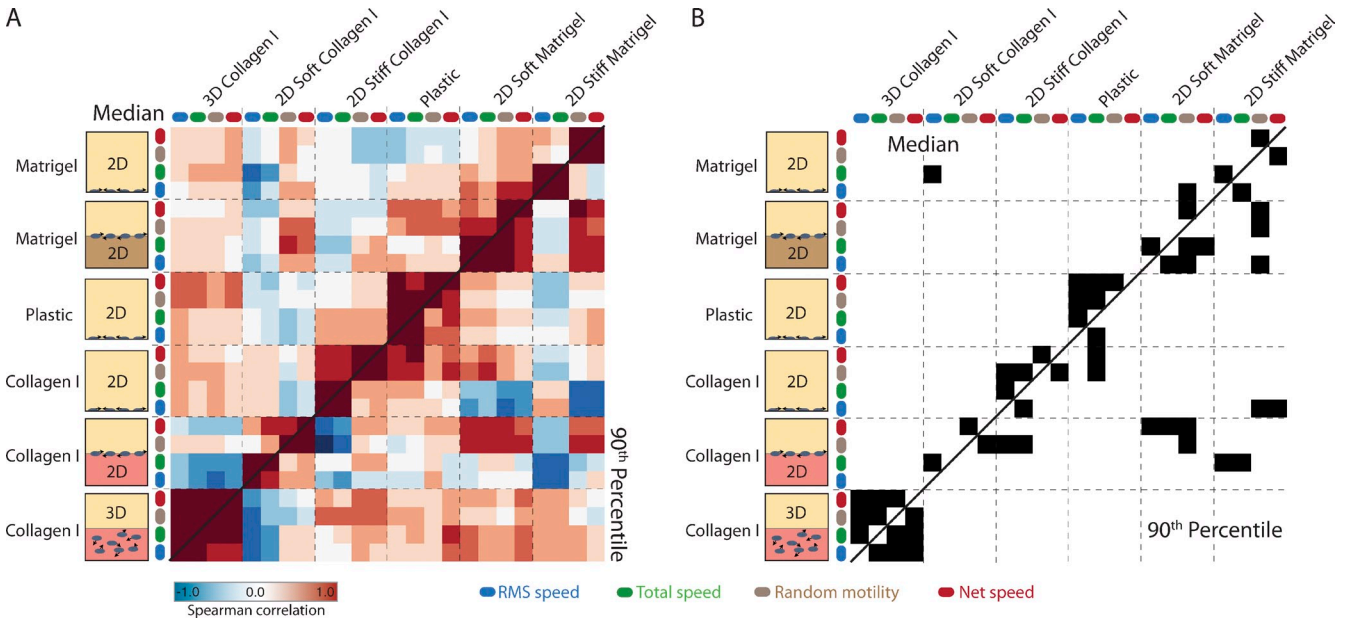

Figure 4. **Motility enhancement in 2D and 3D in MDA-MB-231 is broadly distinct.** (A) All Spearman pairwise correlation coefficients between each motility metric in each 2D and 3D migration assay across growth factor stimuli. The top and bottom diagonals show coefficients corresponding to the median and 90th percentile response profiles, respectively. Arrows show cell movement. (B) Significant correlations ($P < 0.05$) are indicated in black. Correlations are observed along the diagonal between motility metrics but not between different migration assays and 3D migration.

2009; Fraley et al., 2010). However, although migration in vivo is driven by autocrine and paracrine growth factor cues, the effects of growth factor stimulation have not been compared in different dimensional contexts. It is conceivable that growth factor motility responses may be similar in distinct dimensional contexts if various migration-related processes (e.g., protrusion, proteolysis, and retraction) are similarly modulated by growth factor cues.

To study the contributions of dimensional and matrix context on cell migration in vitro systematically, we performed all pairwise comparisons of growth factor–enhanced cell motility metrics in MDA-MB-231 cells (Fig. 4 A). A stronger correlation exists between different motility metrics within a single dimensional or matrix type, reflected by analysis for significant correlations ($P < 0.05$; Fig. 4 B), which only exist within, and not across, dimensionalities.

Here, we systematically demonstrate for the first time that growth factor–enhanced motility is distinct between dimensional contexts. This difference holds serious implications for studies investigating migration in general and, in particular, for analyzing intracellular signaling events that promote migration.

Early protrusion is a better surrogate for measurement of 3D migration response

Next, we sought to identify biophysical processes that may better reflect growth factor–enhanced 3D motility. Within seconds after growth factor stimulation, cells respond through actin polymerization and lamellipodia protrusion, which can be measured in 2D as an area change (Mouneimne et al., 2004). We hypothesized that initial 2D protrusion may reflect eventual motility enhancement in 3D, particularly as 2D protrusion enhancement correlates with metastatic capacity and migration metrics in vivo in one case (Philippar et al., 2008; Roussos et al., 2011).

Acute changes in the area of MDA-MB-231 cells after growth factor stimulation were quantified (Fig. 5 A). This profile of growth factor response (the 50th, 90th, or 95th quantile area change across growth factors) was then compared with that of each motility metric in differing dimensional contexts. We found that lamellipodial protrusion correlates positively with 3D migration (Fig. 5 B). Upon comparison to all 2D motility and protrusion assays, 3D migration correlated better with the acute membrane protrusion response than with any 2D migration measurements (Fig. 5 C). The generality of the link between migration in 3D and early protrusion was tested independently by measuring protrusion across all growth factor conditions in MDA-MB-157 cells (Fig. 5 A). Significant association between 3D migration and lamellipodial protrusion was once again observed despite differences in the growth factor responses between the two cell lines (Figs. 5 D and 2 A). This test is especially stringent, as it requires similarity across growth factors that promote different intracellular signaling responses (Kim et al., 2011).

To more stringently test our observed link between initial protrusion and eventual migration in 3D, as well as to evaluate whether protrusion plays a specific causal role in 3D migration or is simply an auspicious measure of signaling, we selected three drugs that disrupt cytoskeletal elements to test whether 2D migration or protrusion would better predict eventual 3D migration. Notably, drugs that block migration in both 2D and 3D would not address our prediction because we sought to assess the ability of protrusion to evaluate 3D migratory capacity specifically. Nocodazole and blebbistatin were selected for their

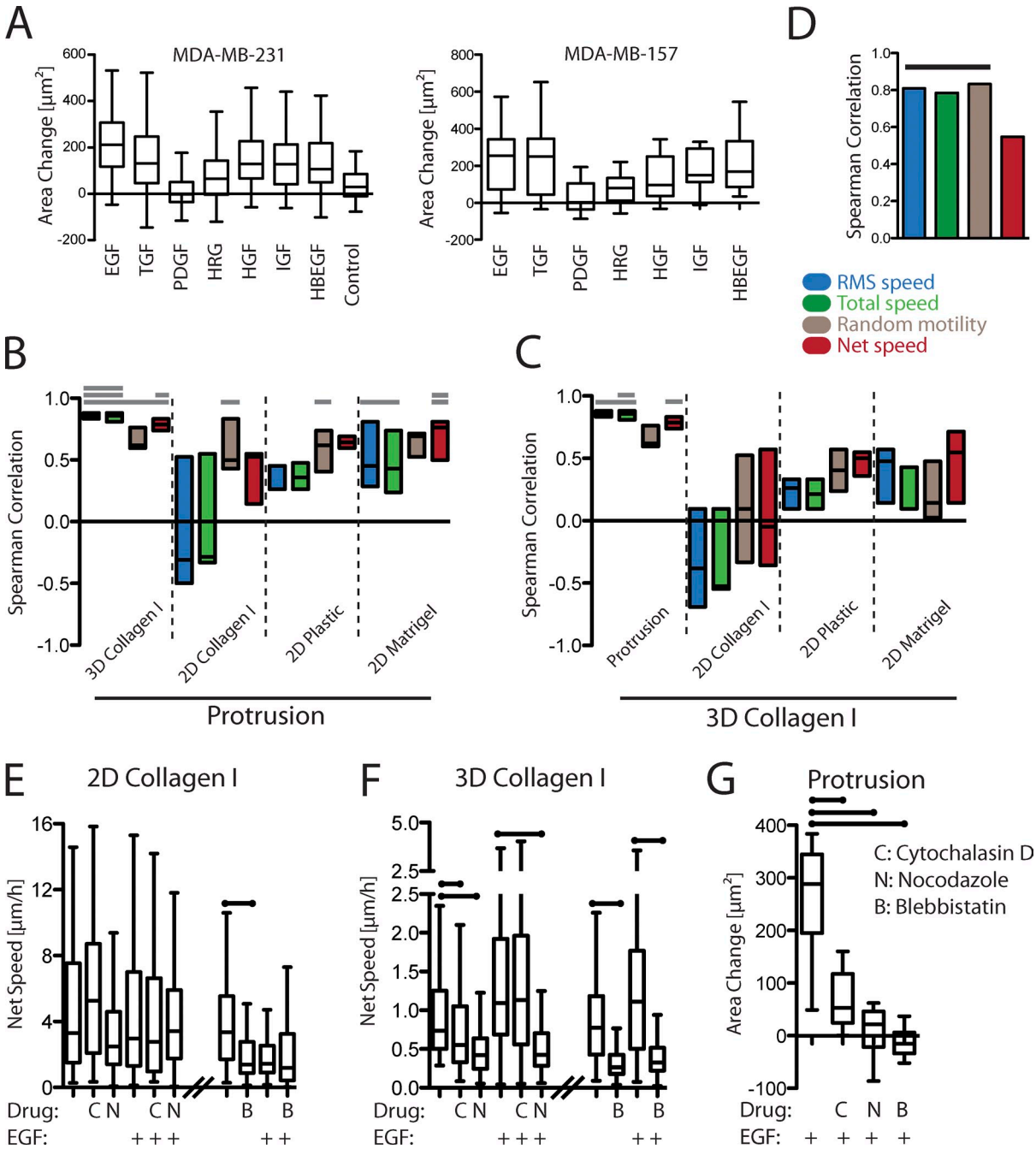

Figure 5. **Protrusion correlates specifically with 3D motility enhancement.** (A) MDA-MB-231 and MDA-MB-157 cells were stimulated with each growth factor condition, and the fold change in cell area was calculated by manual tracing of DIC images (MDA-MB-231, $n = 60–138$; MDA-MB-157, $n = 15–25$ from at least three independent experiments). (B) Rank correlation coefficients were calculated for MDA-MB-231 between the median, 90th percentile, and 95th percentile protrusion responses and the migration responses across different metrics of migration and assays. Each box is bounded by the highest and lowest correlation calculated, with a line indicating the median correlation calculated. Bars on the top indicate the number of quantiles for which the correlation is significant (Storey correction, $q < 0.05$; 0.75 false positive). (C) Similar analysis shows correlations between 3D motility and protrusion or different 2D motility assays ($q < 0.05$; 0.2 false positive). (D) Protrusion and 3D motility also correlate in MDA-MB-157 cells. Bar indicates correlations that are significantly nonzero ($P < 0.05$). (E) Net displacement of MDA-MB-231 cells treated with three cytoskeleton-related inhibitors with or without EGF stimulation on stiff collagen matrix. (F) Net displacement of cells treated similarly within 3D collagen gels. (G) Protrusion in response to EGF stimulation for cells treated with each cytoskeletal drug. For inhibitor experiments, a single representative experiment is shown. An independent replicate showed qualitatively identical results but was not quantified. (E–G) Bars on the top indicate significant differences with respect to the no inhibitor control ($P < 0.05$). (A and E–G) The lines indicate the median. The box is bound by the 25th and 75th quantiles. The whiskers extend to either the maximum and minimum values or three halves the interquartile range, depending on which is closer to the median. IGF, insulin-like growth factor 1; HRG, Heregulin β1; HBEGF, heparin-binding EGF-like growth factor; HGF, hepatocyte growth factor.

documented distinct effects in 2D and 3D contexts (Doyle et al., 2009), whereas cytochalasin D was chosen for its ability at low doses to reduce barbed-end elongation of actin filaments (Bear et al., 2002). MDA-MB-231 cells were treated with the three drugs with or without EGF stimulation on stiff collagen in 2D (Figs. 5 E and S2 A) or in 3D collagen gels (Figs. 5 F and S2 B). In parallel, initial protrusion was evaluated as before (Fig. 5 G). Whereas 2D migration was not affected by any of these three drug treatments under EGF stimulation conditions (Fig. 5 E), EGF-induced 3D migration was noticeably decreased by nocodazole and blebbistatin (Fig. 5 F). These decreases corresponded well to strongly diminished EGF-elicited protrusion response for both these two drugs (Fig. 5 G). The effect of cytochalasin D on EGF-elicited protrusion was milder than for nocodazole and blebbistatin, so the lack of significant reduction of 3D migration serves as at least an intermediate correspondence for this third drug.

Our results ought not be taken to imply that modulation of membrane protrusion dynamics be considered to necessarily be the sole, or even predominant, governing mechanism for motility enhancement in response to growth factor stimuli. Strong evidence exists indicating that 3D migration is concomitantly modulated by other processes, such as traction and proteolysis. Focal proteolysis in 3D collagen gels has been suggested to be driven by pericellular constriction resulting from pseudopodial protrusion, promoting integrin- and membrane-associated protease clustering (Wolf et al., 2007). Whether by functional or phenomenological means, protrusion frequency and matrix deformation correlate significantly in 3D collagen (Fraley et al., 2010). However, interpretation of results obtained from probing protease function by biochemical or genetic means is complicated by the effects of proteases on growth factor ligand and receptor shedding along with their effects on matrix degradation. Thus, mechanistic relationships for convoluted effects of protease activities between membrane protrusion and migration will remain extremely difficult to parse until quantitative multivariate measurement and analysis technologies (e.g., Miller et al., 2011) can be applied across broad treatment landscapes. Importantly, the correspondence found here between acute actin polymerization responses and longer term 3D migration response in response to growth factor stimulation offers an opportunity for more vigorous investigation of intracellular signaling pathways regulating 3D migration. Biochemical analyses from or on a plate of sparsely seeded cells with enough physical space for robust membrane protrusion are much more tractable than collection of cells or real-time analysis of signaling events within cells in a 3D matrix.

As migration within 3D was only observed with cells of one clinical subtype (ER−/PR−/HER2 normal), our observation of correspondence between short-term protrusion and migration in 3D remains to be tested for cells of other clinical subtypes and lineages. However, although bulk tumors may not be represented by the cell lines of mesenchymal phenotype, metastasis-relevant subpopulations may show a distinct expression signature (Giampieri et al., 2009). Our results urge consideration of protrusion measurement, at least over measurement of 2D motility, as an indicator of 3D migration-relevant response.

A detailed mechanistic picture describing the modulation of multiple essential processes involved in interstitial migration remains to be constructed, with careful consideration of intricate forms of cross talk between these processes being an important key. Here, we have presented a systematic deconstruction of migration behaviors across an especially invasive and lethal subtype of breast cancer. Our findings point toward the initial steps in actin polymerization–driven membrane protrusion as an important regulator of invasive potential in these cells. Our contribution offers an improved basis for rational experimental design and pinpoints the time scale that may be most relevant for quantification. As migration in vivo may occur via directed paracrine cues from tumor-associated cell populations, high-throughput analyses of migration responses to growth factor cues are likely to reveal effective targets of metastatic suppression.

Materials and methods

Antibody reagents, growth factors, and inhibitors

Antibodies against EGFR, IGF1R, C-Met, and glyceraldehyde 3-phosphate dehydrogenase (GAPDH) were purchased from Cell Signaling Technology. EGF, PDGF-BB, and TGF-α were purchased from Invitrogen. IGF1, hepatocyte growth factor, heparin-binding EGF-like growth factor, and Heregulin β1 were purchased from PeproTech. EGF and IGF1 were used at 100 ng/ml, Heregulin β1 was used at 80 ng/ml, and all others were used at 50 ng/ml for all experiments. (S)-(-)-Blebbistatin, cytochalasin D, and nocodazole were purchased from Santa Cruz Biotechnology, Inc. and used at 50 µM, 25 nM, and 10 µM, respectively.

Cell culture

MDA-MB-231, BT-549, and MDA-MB-157 cells were cultured in high-glucose DME supplemented with 10% FBS and 1% penicillin–streptomycin. SUM-159 cells were cultured in Ham's F12 media supplemented with 5 µg/ml insulin (Lonza), 1 µg/ml hydrocortisone (BD), 5% FBS, and 1% penicillin–streptomycin.

Migration analysis

For 3D migration assessment, cells were labeled with CMPTX (Invitrogen) for 20 min and mixed with 2.2 mg/ml pH-neutralized, acid-extracted, nonpepsin digested collagen I (BD) with DME at 500,000 cells/ml. The matrix–cell solution was placed in a glass-bottom multiwell plate (MatTek), polymerized for 30 min at 37°C, and then overlaid with full serum media overnight. Cells were stimulated 4 h before imaging on an environment-controlled microscope (TE2000; Nikon) with a camera (C4742-95-12ERG; Hamamatsu Photonics) and a Plan Apochromat 10× 0.45 NA differential interference contrast (DIC) L air objective. Image stacks of 70 3-µm slices were obtained every 60 min for 16 h using MetaMorph (Molecular Devices). Where indicated, inhibitors were added simultaneously to stimulation. To avoid artifacts caused by potential gradients in stiffness near the edges of the gel, analysis fields were selected >200 µm from the glass surface.

For soft 2D migration assays, 100 µl pH-neutralized, acid-extracted 2.2 mg/ml collagen I or 100% matrigel was spread across wells of a 48-well plate and allowed to polymerize. For stiff 2D migration assays, either 100 µg/ml collagen I in 20 mM acetic acid or 0.2% matrigel in serum-free medium was used to coat uncoated glass multiwall plates for 30 min (MatTek). Cells were then labeled with CMFDA (Invitrogen) for 20 min and seeded sparsely on wells with matrix or directly on tissue-culture plastic. The next day, cells were stimulated 4 h before imaging every 10 min for 16 h. Where indicated, inhibitors were added simultaneously to stimulation.

Cells were tracked using Imaris (Bitplane). From each track, the RMS cell speed was calculated from position intervals between time points as well as the standard deviation of the mean. Total and net speeds were calculated by dividing the total path length and net displacement by the duration of the experiment. Each track was then fit to a random walk model using the method of nonoverlapping intervals as previously described to calculate the random motility coefficient (Kim et al., 2008). In brief, individual cell

speeds were calculated from each track using the mean of each time interval. Mean squared displacements were then calculated as the mean squared distance of all nonoverlapping intervals within a track. Using the mean squared displacement (MSD) for varying time intervals, the following equation was fit using least squares to yield a fit persistence:

$$MSD = 2S^2P\left[t - P\left(1 - e^{-t/P}\right)\right].$$

From the fit, the random motility coefficient (RMC) was calculated as $RMC = S^2P$, analogously to the diffusion coefficient (S, speed; P, persistence; t, time).

Protrusion assays

Glass-bottomed dishes (MatTek) were coated with 0.2% matrigel in serum-free media for 30 min. Cells were seeded sparsely overnight and then serum starved for 4 h in L15 media with 0.35% bovine serum albumin. Inhibitors, when indicated, were added at the beginning of serum starvation. DIC images were acquired every 10 s for 1 min before stimulation and 9 min after stimulation. Cell areas were traced immediately before stimulation and 9 min after stimulation using ImageJ (National Institutes of Health). Single-cell information was aggregated from at least three independent experiments.

Receptor expression and activation measurement

Cells were plated sparsely on 15-cm plates overnight, washed with PBS, and lysed with 500 µl of radioimmunoprecipitation assay buffer containing protease inhibitor (Roche) and phosphatase inhibitor cocktail (Boston BioProducts). Equal protein was loaded for SDS-PAGE analysis using a bicinchoninic acid assay and blotted using standard techniques with antibodies against GAPDH, EGFR, IGF1R, and C-Met. Densitometry was performed on an imager (Odyssey; LI-COR Biosciences) and normalized to GAPDH as a loading control.

For activation measurement, cells were seeded sparsely overnight and starved for 4 h the next day followed by stimulation with either 100 ng/ml EGF or 50 ng/ml TGF-α for 5 min. Cells were lysed using lysis buffer (Bio-Rad Laboratories) containing protease inhibitor (Roche) and phosphatase inhibitor cocktail (Boston BioProducts). EGFR pan-pY was measured using a bead-based ELISA assay (Bio-Rad Laboratories) loaded with equal protein using a bicinchoninic acid assay. Linearity of the assay with respect to protein concentration was verified.

Numerical analysis

All analysis was performed in MATLAB (MathWorks). Single-cell data from each experiment were imported, and each quantile of interest (50th, 90th, or 95th) was calculated for each motility metric and condition. Each set of growth factor conditions within a given quantile was then normalized to the condition absent of growth factor stimulation (or mean centered if indicated). The mean and standard error were then calculated from independent experiments. Comparisons of motility metrics between single growth factor conditions were performed using the Student's *t* test or the Mann–Whitney test for single-cell data.

For single cell–based migration parameter clustering, Spearman correlation (ρ) of the parameters for individual cells from all experiments for a single cell line in 3D ($n \geq 3$) were calculated and used to calculate pairwise distances, in which perfect correlation corresponds to a distance of zero, and anticorrelation corresponds to a distance of two ($1 - \rho$). Multidimensional scaling in two dimensions captured >99% of the distance quantities for all cell lines. The first principle component captured 90–95% of the distance quantities, whereas the second principle component captured 5–10%. Standard error was calculated by jackknife, during which each cell was removed separately, and each time, both the distances and scaling repeated (Efron and Gong, 1983). For clustering of quantile-level migration metrics, each growth factor profile was mean centered and averaged across experimental replicates. Clustering of profiles and growth factors was performed by rank correlation and mean linkage.

Receptor expression and motility enhancement comparison were tested for significance using the binomial distribution. Where indicated, motility enhancement was variance normalized between cell lines by log transformation (so as to center fold-change values around zero) and by division by the standard deviation across growth factor conditions.

Growth factor profiles were compared by calculating the Spearman correlation, and significance was calculated by permutation. Where many comparisons were performed, multiple hypothesis testing was performed as indicated. When comparing migration in 2D and 3D contexts, multiple hypothesis correction was not performed, as type I error is not a concern. When comparing protrusion and 3D migration results, identical quantiles of single-cell data were always used.

Online supplemental material

Fig. S1 shows an example of fluorescent stacks from a 3D migration assay and preliminary analysis of the migration phenotypes. Fig. S2 shows the RMS speed measurements for the experiments shown in Fig. 5 (E and F). Table S1 shows the subtype characteristics of each cell line examined and whether it was observed to migrate in 3D. Online supplemental material is available at http://www.jcb.org/cgi/content/full/jcb.201201003/DC1.

This work was supported by the National Institutes of Health (grants R01-GM081336 to D.A. Lauffenburger and A. Wells and U54-CA112967 to D.A. Lauffenburger and F.B. Gertler), the National Science Foundation (Graduate Research Fellowship to A.S. Meyer), and the Congressionally Directed Medical Research Programs Department of Defense Breast Cancer Research Program (grants W81XWH-11-1-0088 to A.S. Meyer and W81XWH-10-1-0040 to S.K. Hughes-Alford).

Submitted: 2 January 2012
Accepted: 8 May 2012

References

Al-Hajj, M., M.S. Wicha, A. Benito-Hernandez, S.J. Morrison, and M.F. Clarke. 2003. Prospective identification of tumorigenic breast cancer cells. *Proc. Natl. Acad. Sci. USA*. 100:3983–3988. http://dx.doi.org/10.1073/pnas.0530291100

Bear, J.E., T.M. Svitkina, M. Krause, D.A. Schafer, J.J. Loureiro, G.A. Strasser, I.V. Maly, O.Y. Chaga, J.A. Cooper, G.G. Borisy, and F.B. Gertler. 2002. Antagonism between Ena/VASP proteins and actin filament capping regulates fibroblast motility. *Cell*. 109:509–521. http://dx.doi.org/10.1016/S0092-8674(02)00731-6

Bernards, R., and R.A. Weinberg. 2002. A progression puzzle. *Nature*. 418:823. http://dx.doi.org/10.1038/418823a

Charafe-Jauffret, E., C. Ginestier, F. Monville, P. Finetti, J. Adélaïde, N. Cervera, S. Fekairi, L. Xerri, J. Jacquemier, D. Birnbaum, and F. Bertucci. 2006. Gene expression profiling of breast cell lines identifies potential new basal markers. *Oncogene*. 25:2273–2284. http://dx.doi.org/10.1038/sj.onc.1209254

Cheng, N., N.A. Bhowmick, A. Chytil, A.E. Gorksa, K.A. Brown, R. Muraoka, C.L. Arteaga, E.G. Neilson, S.W. Hayward, and H.L. Moses. 2005. Loss of TGF-β type II receptor in fibroblasts promotes mammary carcinoma growth and invasion through upregulation of TGF-α-, MSP- and HGF-mediated signaling networks. *Oncogene*. 24:5053–5068. http://dx.doi.org/10.1038/sj.onc.1208685

Cheng, N., A. Chytil, Y. Shyr, A. Joly, and H.L. Moses. 2008. Transforming growth factor-β signaling-deficient fibroblasts enhance hepatocyte growth factor signaling in mammary carcinoma cells to promote scattering and invasion. *Mol. Cancer Res.* 6:1521–1533. http://dx.doi.org/10.1158/1541-7786.MCR-07-2203

Cristofanilli, M., G.T. Budd, M.J. Ellis, A. Stopeck, J. Matera, M.C. Miller, J.M. Reuben, G.V. Doyle, W.J. Allard, L.W. Terstappen, and D.F. Hayes. 2004. Circulating tumor cells, disease progression, and survival in metastatic breast cancer. *N. Engl. J. Med.* 351:781–791. http://dx.doi.org/10.1056/NEJMoa040766

Doyle, A.D., F.W. Wang, K. Matsumoto, and K.M. Yamada. 2009. One-dimensional topography underlies three-dimensional fibrillar cell migration. *J. Cell Biol.* 184:481–490. http://dx.doi.org/10.1083/jcb.200810041

Dunn, M., P. Sinha, R. Campbell, E. Blackburn, N. Levinson, R. Rampaul, T. Bates, S. Humphreys, and W.J. Gullick. 2004. Co-expression of neuregulins 1, 2, 3 and 4 in human breast cancer. *J. Pathol.* 203:672–680. http://dx.doi.org/10.1002/path.1561

Efron, B., and G. Gong. 1983. A leisurely look at the bootstrap, the jackknife, and cross-validation. *Am. Stat.* 37:36–48.

Fraley, S.I., Y. Feng, R. Krishnamurthy, D.-H. Kim, A. Celedon, G.D. Longmore, and D. Wirtz. 2010. A distinctive role for focal adhesion proteins in three-dimensional cell motility. *Nat. Cell Biol.* 12:598–604. http://dx.doi.org/10.1038/ncb2062

Friedl, P., and K. Wolf. 2009. Proteolytic interstitial cell migration: a five-step process. *Cancer Metastasis Rev.* 28:129–135. http://dx.doi.org/10.1007/s10555-008-9174-3

Giampieri, S., C. Manning, S. Hooper, L. Jones, C.S. Hill, and E. Sahai. 2009. Localized and reversible TGFbeta signalling switches breast cancer cells from cohesive to single cell motility. *Nat. Cell Biol.* 11:1287–1296. http://dx.doi.org/10.1038/ncb1973

Goswami, S., E. Sahai, J.B. Wyckoff, M. Cammer, D. Cox, F.J. Pixley, E.R. Stanley, J.E. Segall, and J.S. Condeelis. 2005. Macrophages promote the invasion of breast carcinoma cells via a colony-stimulating factor-1/epidermal growth factor paracrine loop. *Cancer Res.* 65:5278–5283. http://dx.doi.org/10.1158/0008-5472.CAN-04-1853

Hankinson, S.E., W.C. Willett, G.A. Colditz, D.J. Hunter, D.S. Michaud, B. Deroo, B. Rosner, F.E. Speizer, and M. Pollak. 1998. Circulating concentrations of insulin-like growth factor-I and risk of breast cancer. *Lancet*. 351:1393–1396. http://dx.doi.org/10.1016/S0140-6736(97)10384-1

Hutcheson, I.R., J.M. Knowlden, S.E. Hiscox, D. Barrow, J.M. Gee, J.F. Robertson, I.O. Ellis, and R.I. Nicholson. 2007. Heregulin β1 drives gefitinib-resistant growth and invasion in tamoxifen-resistant MCF-7 breast cancer cells. *Breast Cancer Res.* 9:R50. http://dx.doi.org/10.1186/bcr1754

Jin, Q., and F.J. Esteva. 2008. Cross-talk between the ErbB/HER family and the type I insulin-like growth factor receptor signaling pathway in breast cancer. *J. Mammary Gland Biol. Neoplasia*. 13:485–498. http://dx.doi.org/10.1007/s10911-008-9107-3

Kim, H.-D., T.W. Guo, A.P. Wu, A. Wells, F.B. Gertler, and D.A. Lauffenburger. 2008. Epidermal growth factor-induced enhancement of glioblastoma cell migration in 3D arises from an intrinsic increase in speed but an extrinsic matrix- and proteolysis-dependent increase in persistence. *Mol. Biol. Cell*. 19:4249–4259. http://dx.doi.org/10.1091/mbc.E08-05-0501

Kim, H.-D., A.S. Meyer, J.P. Wagner, S.K. Alford, A. Wells, F.B. Gertler, and D.A. Lauffenburger. 2011. Signaling network state predicts twist-mediated effects on breast cell migration across diverse growth factor contexts. *Mol. Cell. Proteomics*. 10:M111:008433–1–M111:008433–12. http://dx.doi.org/10.1074/mcp.M111.008433

Kipper, M.J., H.K. Kleinman, and F.W. Wang. 2007. New method for modeling connective-tissue cell migration: improved accuracy on motility parameters. *Biophys. J.* 93:1797–1808. http://dx.doi.org/10.1529/biophysj.106.096800

Lara, R., F.A. Mauri, H. Taylor, R. Derua, A. Shia, C. Gray, A. Nicols, R.J. Shiner, E. Schofield, P.A. Bates, et al. 2011. An siRNA screen identifies RSK1 as a key modulator of lung cancer metastasis. *Oncogene*. 30:3513–3521. http://dx.doi.org/10.1038/onc.2011.61

Lauffenburger, D.A., and A.F. Horwitz. 1996. Cell migration: a physically integrated molecular process. *Cell*. 84:359–369. http://dx.doi.org/10.1016/S0092-8674(00)81280-5

Lazebnik, Y. 2010. What are the hallmarks of cancer? *Nat. Rev. Cancer*. 10:232–233. http://dx.doi.org/10.1038/nrc2827

Mader, C.C., M. Oser, M.A.O. Magalhaes, J.J. Bravo-Cordero, J. Condeelis, A.J. Koleske, and H. Gil-Henn. 2011. An EGFR-Src-Arg-cortactin pathway mediates functional maturation of invadopodia and breast cancer cell invasion. *Cancer Res.* 71:1730–1741. http://dx.doi.org/10.1158/0008-5472.CAN-10-1432

McIntyre, E., E. Blackburn, P.J. Brown, C.G. Johnson, and W.J. Gullick. 2010. The complete family of epidermal growth factor receptors and their ligands are co-ordinately expressed in breast cancer. *Breast Cancer Res. Treat.* 122:105–110. http://dx.doi.org/10.1007/s10549-009-0536-5

Miller, M.A., L. Barkal, K. Jeng, A. Herrlich, M. Moss, L.G. Griffith, and D.A. Lauffenburger. 2011. Proteolytic Activity Matrix Analysis (PrAMA) for simultaneous determination of multiple protease activities. *Integr. Biol. (Camb.)*. 3:422–438. http://dx.doi.org/10.1039/c0ib00083c

Mograbi, B., N. Rochet, V. Imbert, I. Bourget, R. Bocciardi, C. Emiliozzi, and B. Rossi. 1997. Human monocytes express amphiregulin and heregulin growth factors upon activation. *Eur. Cytokine Netw.* 8:73–81.

Mouneimne, G., L. Soon, V. DesMarais, M. Sidani, X. Song, S.-C. Yip, M. Ghosh, R. Eddy, J.M. Backer, and J. Condeelis. 2004. Phospholipase C and cofilin are required for carcinoma cell directionality in response to EGF stimulation. *J. Cell Biol.* 166:697–708. http://dx.doi.org/10.1083/jcb.200405156

Pasanisi, P., E. Venturelli, D. Morelli, L. Fontana, G. Secreto, and F. Berrino. 2008. Serum insulin-like growth factor-I and platelet-derived growth factor as biomarkers of breast cancer prognosis. *Cancer Epidemiol. Biomarkers Prev.* 17:1719–1722. http://dx.doi.org/10.1158/1055-9965.EPI-07-0654

Philippar, U., E.T. Roussos, M. Oser, H. Yamaguchi, H.-D. Kim, S. Giampieri, Y. Wang, S. Goswami, J.B. Wyckoff, D.A. Lauffenburger, et al. 2008. A Mena invasion isoform potentiates EGF-induced carcinoma cell invasion and metastasis. *Dev. Cell*. 15:813–828. http://dx.doi.org/10.1016/j.devcel.2008.09.003

Roussos, E.T., M. Balsamo, S.K. Alford, J.B. Wyckoff, B. Gligorijevic, Y. Wang, M. Pozzuto, R. Stobezki, S. Goswami, J.E. Segall, et al. 2011. Mena invasive (MenaINV) promotes multicellular streaming motility and transendothelial migration in a mouse model of breast cancer. *J. Cell Sci.* 124:2120–2131. http://dx.doi.org/10.1242/jcs.086231

Simpson, K.J., L.M. Selfors, J. Bui, A. Reynolds, D. Leake, A. Khvorova, and J.S. Brugge. 2008. Identification of genes that regulate epithelial cell migration using an siRNA screening approach. *Nat. Cell Biol.* 10:1027–1038. http://dx.doi.org/10.1038/ncb1762

Tyan, S.W., W.H. Kuo, C.K. Huang, C.C. Pan, J.Y. Shew, K.J. Chang, E.Y. Lee, and W.H. Lee. 2011. Breast cancer cells induce cancer-associated fibroblasts to secrete hepatocyte growth factor to enhance breast tumorigenesis. *PLoS ONE*. 6:e15313. http://dx.doi.org/10.1371/journal.pone.0015313

Weigelt, B., J.L. Peterse, and L.J. van't Veer. 2005. Breast cancer metastasis: markers and models. *Nat. Rev. Cancer*. 5:591–602. http://dx.doi.org/10.1038/nrc1670

Wilson, T.R., D.Y. Lee, L. Berry, D.S. Shames, and J. Settleman. 2011. Neuregulin-1-mediated autocrine signaling underlies sensitivity to HER2 kinase inhibitors in a subset of human cancers. *Cancer Cell*. 20:158–172. http://dx.doi.org/10.1016/j.ccr.2011.07.011

Wolf, K., Y.I. Wu, Y. Liu, J. Geiger, E. Tam, C. Overall, M.S. Stack, and P. Friedl. 2007. Multi-step pericellular proteolysis controls the transition from individual to collective cancer cell invasion. *Nat. Cell Biol.* 9:893–904. http://dx.doi.org/10.1038/ncb1616

Wolf, K., S. Alexander, V. Schacht, L.M. Coussens, U.H. von Andrian, J. van Rheenen, E. Deryugina, and P. Friedl. 2009. Collagen-based cell migration models in vitro and in vivo. *Semin. Cell Dev. Biol.* 20:931–941. http://dx.doi.org/10.1016/j.semcdb.2009.08.005

Wolf-Yadlin, A., N. Kumar, Y. Zhang, S. Hautaniemi, M. Zaman, H.D. Kim, V. Grantcharova, D.A. Lauffenburger, and F.M. White. 2006. Effects of HER2 overexpression on cell signaling networks governing proliferation and migration. *Mol. Syst. Biol.* 2:54. http://dx.doi.org/10.1038/msb4100094

Yarrow, J.C., G. Totsukawa, G.T. Charras, and T.J. Mitchison. 2005. Screening for cell migration inhibitors via automated microscopy reveals a Rho-kinase inhibitor. *Chem. Biol.* 12:385–395. http://dx.doi.org/10.1016/j.chembiol.2005.01.015

Zaman, M.H., L.M. Trapani, A.L. Sieminski, D. Mackellar, H. Gong, R.D. Kamm, A. Wells, D.A. Lauffenburger, and P. Matsudaira. 2006. Migration of tumor cells in 3D matrices is governed by matrix stiffness along with cell-matrix adhesion and proteolysis. *Proc. Natl. Acad. Sci. USA*. 103:10889–10894. http://dx.doi.org/10.1073/pnas.0604460103